



Role of volumetric parameters obtained from ^{68}Ga -PSMA PET/CT and ^{18}F -FDG PET/CT in predicting overall survival in patients with mCRPC receiving taxane therapy

Yunus Güzel¹ · Halil Kömek^{1,3} · Canan Can¹ · İhsan Kaplan¹ · Nadiye Akdeniz² · Ferat Kepenek¹ · Cihan Gündoğan¹

Received: 19 April 2023 / Accepted: 7 June 2023 / Published online: 18 June 2023
© The Author(s) under exclusive licence to The Japanese Society of Nuclear Medicine 2023

Abstract

Objective The aim of this study was to determine the prognostic role of volumetric parameters and Pro-PET scores obtained from ^{68}Ga -prostate-specific membrane antigen (PSMA) PET/CT and ^{18}F -FDG PET/CT in patients with metastatic castration-resistant prostate cancer (mCRPC) receiving taxane therapy.

Materials and methods The study included 71 patients who underwent simultaneous PSMA and ^{18}F -FDG PET/CT imaging between January 2019 and January 2022, had a Pro-PET score of 3–5 and had received taxane therapy after imaging. ^{18}F -FDG tumor volume (TV-F) and PSMA tumor volume (TV-P) values of the lesions and total lesion glycolysis (TL-G) and total lesion PSMA (TL-P) values of the lesions were calculated on both imaging studies and the effects of these parameters on overall survival (OS) were investigated.

Results The median age of the patients included herein was 71 years (56–89) and the median prostate-specific antigen (PSA) level was 16.4 (0.01–1852 ng/dL). According to the Kaplan–Meier survival analysis, TTV-P ≥ 78.5 , TTL-P ≥ 278.8 , TTV-F ≥ 94.98 , TTL-G ≥ 458.3 , TTV-P + F ≥ 195.45 , TTL-G + P ≥ 855.78 , lymph node (L)TV-F ≥ 3.4 , LFDG-SUV-max ≥ 3.2 , LFDG-SUVmean ≥ 2.25 , LFDG-SUVpeak ≥ 2.55 , and bone (B)TV-F ≥ 51.15 values were found to be prognostic factors in predicting short OS. Multivariate Cox regression analysis showed that a Vscore ≥ 3 (95% confidence interval [CI]: 7.069–98.251, $p < 0.001$) and TTL-G + P ≥ 855.78 (95% CI: 4.878–1037.860, $p = 0.006$) were found to be independent prognostic factors in predicting short OS.

Conclusion Volumetric parameters and Pro-PET scores obtained from ^{68}Ga -PSMA PET/CT and ^{18}F -FDG PET/CT imaging have been shown to have an impact on OS in patients with mCRPC receiving taxane therapy.

Keywords ^{18}F -FDG · ^{68}Ga -PSMA · MTV · TLG · Pro-PET score

Introduction

Prostate cancer (PC) is the most common cancer in men and ranks second in terms of mortality (1). Although PC initially responds to androgen deprivation therapy (ADT), it eventually progresses to metastatic castration-resistant prostate cancer (mCRPC) (2, 3).

Prostate-specific membrane antigen (PSMA), a type II transmembrane glycoprotein, is overexpressed in PC cells compared to normal prostate cells. The intensity of PSMA expression on PC cells is further increased depending on the Gleason score (GS) of PC, tumor aggressiveness, androgen independence, recurrence, and metastatic disease (4).

Gallium-68 (^{68}Ga)-PSMA positron emission tomography/computed tomography (PET/CT) is a widely used imaging modality for primary tumor detection, staging,

✉ Halil Kömek
halilkomek@gmail.com

¹ Department of Nuclear Medicine, Sağlık Bilimleri University Diyarbakir Gazi Yasargil, Training and Research Hospital, Diyarbakir, Turkey

² Department of Medical Oncology, Sağlık Bilimleri University Diyarbakir Gazi Yasargil, Training and Research Hospital, Diyarbakir, Turkey

³ SBÜ, Diyarbakir Gazi Yaşargil Eğitim Ve Araştırma Hastanesi, Nükleer Tıp Kliniği, Üçkuyular Mahallesi, Kayapınar, 21070 Diyarbakir, Turkey

and treatment response assessment in patients with PC (5). However, 5–10% of the lesions in patients with PC may not express PSMA glycoprotein due to some alterations related to DNA damage repair, showing inter- or intra-lesion heterogeneity (4, 6). While PC initially does not show typical glucose uptake, it starts to show high glucose uptake, which is called the Warburg effect, after a series of mutations that occur in later periods (7). However, it has been shown that inhibition of PSMA in patients with mCRPC is positively correlated with a higher uptake of 2-Deoxy-2-[fluorine-18] fluoro-d-glucose (^{18}F -FDG) and this is associated with the upregulation of glucose transporter 1 (8). It has also been reported that patients with mCRPC lesions with ^{18}F -FDG affinity are less differentiated and express lower levels of androgen receptors (AR) (9).

Docetaxel is an agent that has been used in patients with mCRPC for many years and its contribution to survival has been confirmed (10). Cabazitaxel is another anticancer agent used in patients with docetaxel-resistant mCRPC and has been shown to improve overall survival (OS) (11). Although the action mechanism of taxanes is not fully understood, some of their activity is seen in their interaction with androgen signalling at both cytoplasmic and nuclear levels in PC cells, affecting androgen-sensitive regulatory mechanisms (12). However, some of the antitumor activity of taxanes may be due to an androgen-independent mechanism. In recent years, advances in molecular knowledge have led to the understanding that PC is a heterogeneous disease in which androgen-dependent and independent clones coexist (13).

In our study, we aimed to determine the prognostic role of volumetric parameters and lesion-based Pro-PET scores obtained from ^{68}Ga -PSMA PET/CT and ^{18}F -FDG PET/CT in predicting OS in patients with mCRPC receiving taxane therapy.

Materials and methods

Study design and patient selection

A total of 391 patients who underwent ^{18}F -FDG PET/CT and ^{68}Ga -PSMA PET/CT at our clinic between January 2019 and January 2022 were retrospectively reviewed. The imaging protocols were performed with a median interval of 3 days (1–7 days) between ^{68}Ga -PSMA and ^{18}F -FDG imaging. All patients underwent ^{68}Ga -PSMA PET/CT followed by ^{18}F -FDG PET/CT.

Patients without ^{68}Ga -PSMA PET/CT or ^{18}F -FDG PET/CT imaging, patients with a Pro-PET score between 0 and 2, patients who did not receive docetaxel and cabazitaxel or whose treatment was incomplete, patients receiving combination therapy (^{177}Lu -PSMA plus taxane), patients with

additional malignancies, patients who died of other causes, and patients whose data were unavailable were excluded.

A total of 71 patients diagnosed with mCRPC who had a Pro-PET score of 3–5 and who were referred to taxane and taxane plus treatments by the oncology board and who had completed docetaxel or cabazitaxel treatment were included in the study (Fig. 1). Docetaxel 75 mg/m^2 or cabazitaxel 25 mg/m^2 , in combination with prednisone $5\text{ mg } 2 \times 1$, was administered every 21 days for a median of six cycles. ADT treatment was continued if castration-resistant. Serum prostate-specific antigen (PSA) levels, GS, and date of death were recorded. Whole-body volumetric parameters were obtained from both imaging studies and recorded. This retrospective study was initiated after approval by the local ethics committee (approval number: 368–2023) and was conducted in accordance with good clinical practice guidelines and current local legislation.

PET/CT protocol

At least 6 h of fasting was recommended prior to ^{18}F -FDG PET/CT imaging and ^{18}F -FDG injection was performed at a dose of 3.5–5.5 MBq/kg with a blood glucose level $< 140\text{ mg/dL}$ measured by the fingerstick method. For ^{68}Ga -PSMA PET/CT imaging, patients received an injection of 2 MBq/kg. All images were acquired using a Discovery IQ 4 ring 20 cm axial field of view (FOV) PET/CT (GE Healthcare, Milwaukee, WI, USA). After injection, whole-body images from the vertex to the mid-thigh were taken at hour 1. After CT images (CT parameters: 120 kV, 80 mAs/slice, 700 mm transaxial FOV, $64 \times 0.625\text{ mm}$ collimation, pitch 1.4, 0.5 s rotation time, 3.3 mm slice thickness, 512×512 matrix), PET images (PET parameters: 3D FOV 20 cm, ordered subset expectation–maximisation algorithm 5 iterations/12 subset, full width at half maximum 3 mm) were acquired at the bed side over 2.5 min in the same position so as to include the same regions. All patients were asked to drink water before PET/CT imaging and urinate immediately before imaging.

Evaluation of images

Images were evaluated consensually by two nuclear medicine physicians with at least 10 years of experience in PET/CT interpretation according to current guidelines (14, 15). After excluding physiologic uptake and false positives, uptakes higher than the mediastinal blood pool were defined as positive for ^{68}Ga -PSMA PET/CT or ^{18}F -FDG PET/CT. Primary tumors and metastatic lesions were counted, measured, and recorded for both imaging modalities. In addition, patients were visually scored according to lesion involvement. According to the Pro-PET scoring system, patients were scored as follows: score 0:

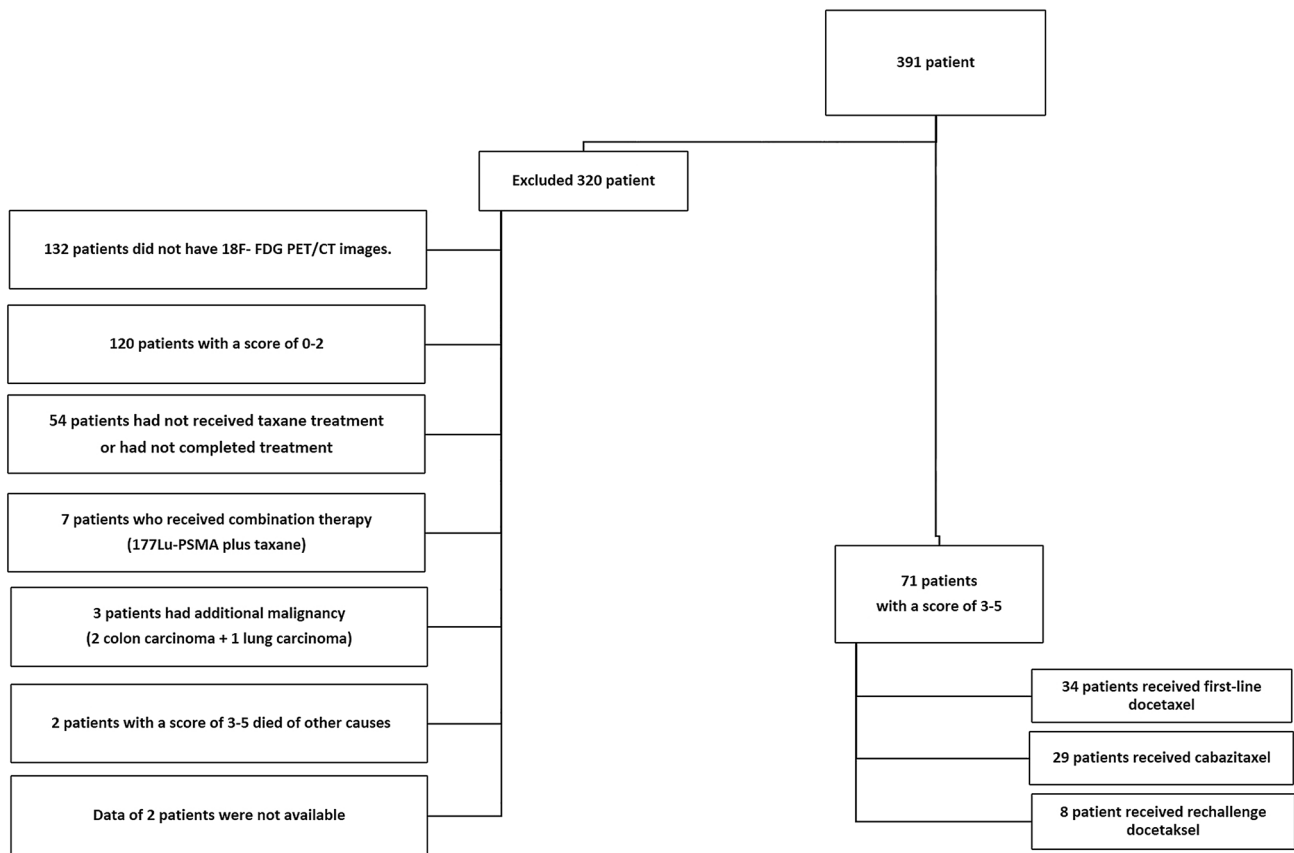


Fig. 1 Patient selection flowchart

PSMA(-) FDG(-), score 1: PSMA(+) FDG(-), score 2: PSMA(+) FDG(+) (FDG < PSMA), score 3: PSMA(+) FDG(+) (FDG = PSMA), score 4: PSMA(+) FDG(+) (FDG > PSMA), score 5: PSMA(-) FDG(+) and recorded accordingly (16). The presence of at least one lesion for any score in organ-based and patient-based evaluation was considered positive for that score. Those with a patient-based score of 3–5 were included in the study.

In both ^{68}Ga -PSMA PET/CT and ^{18}F -FDG PET/CT images of patients with scores of 3–5, semiautomatic VOIs (volume of interest) were drawn from each of the primary lesion and metastatic areas using a 40% SUV threshold, with the lesion within the image area in all three planes.

For primary tumor (P), lymph nodes (L), bone (B), and visceral (V) metastatic lesions, ^{18}F -FDG tumor volume (TV-F) and PSMA tumor volume (TV-P) values of each lesion were automatically provided by the device and these data were summed and recorded as total tumor volume for FDG (TTV-F) and for PSMA (TTV-P). Total lesion glycolysis (TL-G) and total lesion PSMA (TL-P) values for each lesion were calculated and whole body total lesion glycolysis (TTL-G) and whole body total lesion PSMA (TTL-P) values were obtained and recorded. TTV-F and TTV-P

values, which were obtained from ^{18}F -FDG PET/CT and ^{68}Ga -PSMA PET/CT, were added to obtain the whole body total tumor volume FDG + PSMA (TTV-F + P). In addition, TTL-G and TTL-P values were added to obtain the whole body total lesion glycolysis + PSMA (TTL-G + P) value.

Statistical methods

The SPSS 26.0 (IBM Corporation, Armonk, New York, United States) program was used to analyse the variables. The sensitivity and specificity ratios for the relationship between the actual classification and the classification separated by the cut-off value calculated for each variable were examined and expressed by receiver operating characteristic (ROC) curve analysis. Kaplan–Meier (product limit method) log-rank analysis was used to examine the effect of factors on mortality and survival. The univariate and multivariate Cox regression analysis enter method was used to measure the effects of prognostic variables on mortality and survival. Quantitative variables were expressed as mean \pm SD (standard deviation) and median (percentile 25%/percentile 75%), while categorical variables were expressed as n (%).

Variables were analysed with 95% confidence interval (CI) and a p-value less than 0.05 was considered significant.

(78.9%) for visceral metastases (Vscore). The evaluation of lesions based on Pro-PET scoring is shown in Table 1.

Results

The median age of the patients included in the study was 71 (56–89) years. The median serum PSA value was 16.4 (0.01–1852 ng/dl). After imaging, 48% of patients received first-line docetaxel, 11.2% received rechallenged docetaxel and 40.8% received cabazitaxel. Patients receiving rechallenged docetaxel had previously received at least one new generation anti-androgen-axis agent. All patients receiving cabazitaxel had previously received docetaxel and at least one new generation anti-androgen-axis agent. During the study period, 19 patients (26.7%) died, with a median survival of 10.6 months (95% CI: 0.8–47.3).

Pro-PET evaluation showed a score of ≥ 3 in 28 patients (39.5%) for primary prostate lesions (Pscore), 29 patients (40.8%) for lymph node metastases (Lscore), 56 patients (78.9%) for bone metastases (Bscore), and 56 patients

Prognostic factors

Based on the ROC curve analysis, when the TTV-P cut-off value was taken as $\geq 78.5 \text{ cm}^3$, its sensitivity and specificity in predicting mortality were 68% and 67.4%, respectively, which was statistically significant (area under the curve [AUC] = 0.685 ± 0.069 , $P = 0.011$). TTL-P cut-off value ≥ 278.15 , TTV-F cut-off value $\geq 94.95 \text{ cm}^3$, and TTL-G cut-off value ≥ 485.3 were statistically significant in predicting mortality. The cut-off values, AUC, sensitivity and specificity of all parameters are shown in Table 2.

When comparing 1 and 2-year OS rates in Kaplan–Meier survival analysis, Pro-PET Lscore ≥ 3 and Vscore ≥ 3 were found to be prognostic factors predicting short OS ($p = 0.015$ and $p < 0.001$). As quantitative and volumetric assessments, TTV-P ($\geq 78.5 \text{ cm}^3$), TTL-P (≥ 278.8), TTV-F ($\geq 94.98 \text{ cm}^3$), TTL-G (≥ 458.3), TTV-P + F ($\geq 195.45 \text{ cm}^3$), TTL-G + P (≥ 855.78), LTV-FDG (≥ 3.4

Table 1 Evaluation of lesions on imaging based on Pro-PET scoring with ^{68}Ga -PSMA PET/CT and ^{18}F -FDG PET/CT

Score	Prostate		Lymph node		Bone		Visceral	
	N	%	N	%	N	%	N	%
0	12	16.9	34	48	12	16.9	58	81.7
1	8	11.2	2	2.8	0	0	0	0
2	23	32.4	6	8.4	3	4.2	0	0
3	11	15.6	2	2.8	3	4.2	0	0
4	16	22.5	26	36.6	50	70.5	6	8.4
5	1	1.4	1	1.4	3	4.2	7	9.9
Total	71	100	71	100	71	100	71	100

Table 2 ROC curve cut-off, sensitivity, and specificity values in predicting mortality

	Area	Std. Error	p	Asymptotic 95% Confidence Interval		sensitivity (%)	specificity (%)
				Lower Bound	Upper Bound		
TTV-P ≥ 78.5	0.685	0.069	0.011	0.550	0.820	68.00	67.40
TTL-P ≥ 278.15	0.665	0.068	0.022	0.531	0.799	64.00	65.20
TTV-F ≥ 94.95	0.677	0.073	0.015	0.534	0.819	64.00	63.00
TTL-G ≥ 458.3	0.677	0.075	0.014	0.531	0.824	64.00	63.00
TTV-F + P ≥ 195.45	0.692	0.069	0.008	0.558	0.827	64.00	65.20
TTL-G + P ≥ 855.78	0.678	0.070	0.014	0.542	0.815	68.00	69.60
LTV-F ≥ 3.4	0.650	0.069	0.038	0.514	0.786	64.00	63.00
LTL-G ≥ 10.3	0.663	0.070	0.024	0.526	0.799	60.00	61.00
LFDG SUV _{max} ≥ 3.2	0.670	0.069	0.019	0.534	0.806	64.00	63.00
LFDG SUV _{mean} ≥ 2.25	0.662	0.069	0.025	0.526	0.797	64.00	65.20
LFDG SUV _{peak} ≥ 2.55	0.665	0.069	0.022	0.530	0.801	64.00	65.20
BTV-F ≥ 51.15	0.667	0.070	0.021	0.529	0.804	64.00	63.00
BTL-G ≥ 232.15	0.645	0.072	0.045	0.503	0.787	60.00	59.00

T Total. L Lymph node. B Bone

cm³), LFDG-SUV_{max} (≥ 3.2), LFDG-SUV_{mean} (≥ 2.25), LFDG-SUV_{peak} (≥ 2.55) and BTV-F (≥ 51.15 cm³) parameters were found to be prognostic factors predictive of short OS ($p < 0.001$, $p = 0.002$, $p = 0.006$, $p = 0.007$, $p = 0.002$, $p < 0.001$, $p = 0.026$, $p = 0.007$, $p = 0.003$, $p = 0.003$ and $p = 0.006$, respectively) (Table 3).

Univariate Cox regression analysis revealed no statistically significant correlation between age, serum PSA levels, GS, and OS (Table 4). Finally, the multivariate Cox regression analysis showed that a Vscore ≥ 3 (95% CI: 7.069–98.251, $p < 0.001$) and TTL-G + P ≥ 855.78 (95% CI: 4.878–1037.860, $p = 0.006$) were found to be independent prognostic factors predicting short OS (Table 5), (Figs. 2 and 3).

Discussion

In the current study where the measurements are based on the evaluation of both ⁶⁸Ga-PSMA PET/CT and ¹⁸F-FDG PET/CT images, a Vscore of ≥ 3 and the volumetric parameter TTL-G + P of ≥ 855.78 were independent prognostic factors predicting OS in patients with mCRPC receiving taxane therapy.

In the literature, terms such as anaplastic PC, neuroendocrine PC, and intermediate-grade atypical PC, have previously been used for PC with poor prognosis (17). Aggressive variant (AV) PC has been defined in the literature and this newly defined term has been suggested instead of the previous ones (18). It has been reported that AVPC should include at least one of seven features, including the presence of visceral metastasis (19, 20).

There are several studies in the literature on the correlation between volumetric parameters derived from ⁶⁸Ga-PSMA PET/CT and prognosis. Schmuck et al. reported that volumetric parameters may be a quantitative imaging biomarker especially in the evaluation of response to treatment (21). In the study of Grubmüller et al. in which patients with mCRPC receiving different treatments were included, the researchers found that the use of SUV_{mean}, SUV_{max}, SUV_{peak}, and TTV-P parameters derived from ⁶⁸Ga-PSMA-11 PET/CT were suitable for assessing treatment response; however, they found no association with OS (22). In another study that included patients with mCRPC receiving second-generation ADT, pretreatment TTV-P ≥ 124.85 (OR: 11.4, 95% CI 1.11–116, 6, $P = 0.04$) was found to be an independent prognostic factor for OS (23). In a study where Can et al. evaluated patients receiving docetaxel and abiraterone-enzalutamide, TTV-P ≥ 116.88 was reported to be an independent prognostic factor in predicting mortality (24). In another study where Telli et al. studied patients receiving docetaxel and abiraterone-enzalutamide treatments, the researchers found that TTV-P ≥ 40.1 was an

independent prognostic factor for survival (HR: 1.003, 95% CI 1.001–1.004, $p = 0.001$) in multivariate analysis (25). Siefert et al. found that TTV-P level was a negative prognostic factor on OS in their multivariate cox analysis in the group receiving ¹⁷⁷Lu-PSMA ligand treatment (26). In our univariate analysis, TTV-P ≥ 78.5 (95% CI 9.354–15.325) $p < 0.001$ and TTL-P ≥ 278.15 (95% CI 10.055–15.806) $p = 0.002$ were found to be negative prognostic factors for OS. However, in the multivariate analysis, the volumetric parameters obtained from ⁶⁸Ga-PSMA PET/CT alone were not found to be independent prognostic factors.

Normal cells derive energy from glucose through oxidative phosphorylation via the mitochondrial citric acid cycle. Most cancer cells derive their energy from lactic acid fermentation, which synthesises less ATP, even in the presence of oxygen (27). The dense glucose required for these cancer cells is transported into the cell via glucose transporters (GLUTs) (28). ¹⁸F-FDG PET/CT imaging is based on this mechanism (29). However, the role of ¹⁸F-FDG PET/CT imaging in PC is limited (30). It has been shown by immunohistochemical and micro-PET studies that differentiated PC cells take up glucose via sodium-glucose co-transporter 2 (31). Previous studies have shown that androgen increases GLUT1 expression in androgen-dependent PC. This suggests that androgen signalling may play a role in the regulation of GLUT1 (8, 32). However, the mechanisms underlying GLUT1 regulation by androgen signalling remain unclear. GLUT1 is a key mediator of ¹⁸F-FDG uptake into the cell and is associated with the aggressive phenotype of androgen-independent PC (33).

Although mCRPC is a heterogeneous disease, approximately 87% of patients with mCRPC have at least one ¹⁸F-FDG PET/CT positive metastasis (9). Bauckneh et al. found that decreased MTV (MTV < 325.97 cm³) and TLG (TLG < 844.86) values were associated with increased OS. They also reported that MTV was an independent prognostic factor for OS in multivariate analysis (34). In a retrospective study, Wibmer et al. found that TTL-G was independently associated with OS in patients with mCRPC receiving first-line treatment with abiraterone or enzalutamide ($p < 0.001$) and reported that it may qualify as a quantitative prognostic imaging biomarker (35). In our univariate analysis, TTV-F ≥ 94.95 , TTL-G ≥ 458.3 , LTV-F ≥ 3.4 , LTL-G ≥ 10.3 , LFDG-SUV_{max} ≥ 3.2 , LFDG-SUV_{mean} ≥ 2.25 , LFDG-SUV_{peak} ≥ 2.55 , and BTV-F ≥ 51.15 were found to be negative prognostic factors for OS. However, in multivariate analysis, volumetric parameters obtained from ¹⁸F-FDG PET/CT alone were not found to be independent prognostic factors.

In the study by Ferdinandus et al. where they used ¹⁸F-FDG PET/CT and ⁶⁸Ga-PSMA PET/CT together in patients receiving ¹⁷⁷Lu-PSMA therapy, FDG-positive

Table 3 Kaplan meier 1 and 2 year survey analysis

	Mean			P
	E ± Std	95% CI(L-U)	1 and 2 year OS %	
Pscore ≥ 3				
None	25.43 ± 3.75	18.110–32.750	62.5/42.3	0.163
Yes	19.38 ± 1.69	16.050–22.710	85.3/54.9	
Lscore ≥ 3				
None	33.74 ± 3.43	27.017–40.468	82.3/63.6	0.015
Yes	13.80 ± 1.75	10.378–17.240	57.5/20.5	
Bscore ≥ 3				
None	16.13 ± 1.60	13.008–19.248	92.7/27.9	0.447
Yes	28.03 ± 3.14	21.880–34.195	67.5/49.5	
Vscore ≥ 3				
None	31.58 ± 3.11	25.481–37.678	84.7/55.1	<0.001
Yes	6.33 ± 1.396	3.594–9.066	10/10	
TTV-P				
< 78.5	35.71 ± 3.49	28.868–42.569	88.1/66.6	<0.001
≥ 78.5	12.33 ± 1.52	9.354–15.325	53.8/21.2	
TTL-P				
< 278.15	35.25 ± 3.46	28.467–42.035	83.1/66.8	0.002
≥ 278.15	12.93 ± 1.46	10.055–15.806	59.7/20.5	
TTV-F				
< 94.95	34.73 ± 1.56	27.737–41.722	81.7/65.6	0.006
≥ 94.95	13.42 ± 1.49	10.494–16.348	62.5/22.5	
TTL-G				
< 458.3	34.50 ± 3.58	27.474–41.533	80.7/64.6	0.007
≥ 458.3	14.10 ± 1.74	10.672–17.529	63.4/25.9	
TTV-P+F				
< 195.45	35.29 ± 3.43	28.561–42.020	82.3/67.2	0.002
≥ 195.45	12.96 ± 1.49	10.035–15.895	60.9/19.3	
TTL-G+P				
< 855.78	36.32 ± 3.38	29.687–42.971	85.1/69.5	<0.001
≥ 855.78	12.26 ± 1.50	9.312–15.219	56/17.8	
LTV-F				
< 3.4	33.74 ± 3.82	26.241–41.243	86.4/63	0.026
≥ 3.4	14.86 ± 1.68	11.566–18.164	56.8/31.1	
LTL-G				
< 10.3	32.70 ± 3.81	25.222–40.179	82.9/60.5	0.086
≥ 10.3	15.40 ± 1.70	12.067–18.749	60.8/33.4	
LFDG-SUVmax				
< 3.2	34.66 ± 3.57	27.652–41.671	86.4/65.8	0.007
≥ 3.2	13.92 ± 1.66	10.666–17.190	55/22	
LFDG-SUVmean				
< 2.25	35.05 ± 3.48	28.216–41.893	86.7/66.9	0.003
≥ 2.25	13.41 ± 1.64	10.199–16.637	53.1/19	
LFDG-SUVpeak				
< 2.55	35.05 ± 3.48	28.216–41.893	86.7/66.9	0.003
≥ 2.55	13.41 ± 1.64	10.199–16.637	53.1/19	
BTV-F				
< 51.15	34.64 ± 3.56	27.650–41.639	81.1/65	0.006
≥ 51.15	13.28 ± 1.53	10.290–16.289	60.2/22.8	
BTLG-F				

Table 3 (continued)

	Mean			
	E ± Std	95% CI(L-U)	1 and 2 year OS %	P
< 232.15	32.1 ± 3.91	24.427–39.786	76.8/58.5	0.131
≥ 232.15	14.84 ± 1.49	11.911–17.781	68.6/35.3	
Overall	28.19 ± 2.88	22.534–33.847		

T Total. P Prostate. L Lymph node. B Bone. V Visseral

Table 4 Univariate analyses of factors for predicting overall survival

	OR	95.0% CI		p
		Lower	Upper	
Age	1.035	0.984	1.089	0.186
PSA (ng/ml)	1.000	0.999	1.000	0.546
GS Total	1.264	0.874	1.828	0.214
Pscore ≥ 3	0.553	0.238	1.287	0.169
Lscore ≥ 3	2.600	1.170	5.776	0.019
Bscore ≥ 3	1.515	0.515	4.452	0.450
Vscore ≥ 3	8.331	3.510	19.776	0.000
TTV-P ≥ 78.5	4.405	1.871	10.370	0.001
TTL-P ≥ 278.15	3.402	1.480	7.824	0.004
TTV-F ≥ 94.95	2.977	1.308	6.776	0.009
TTL-G ≥ 458.3	2.923	1.287	6.637	0.010
TTV-P + F ≥ 195.45	3.390	1.488	7.725	0.004
TTL-G + P ≥ 855.78	4.375	1.878	10.190	0.001
LTV-F ≥ 3.4	2.458	1.083	5.576	0.031
LTL-G ≥ 10.3	1.994	0.893	4.453	0.092
LFDG-SUVmax ≥ 3.2	2.955	1.290	6.769	0.010
LFDG-SUVmean ≥ 2.25	3.288	1.434	7.540	0.005
LFDG-SUVpeak ≥ 2.55	3.288	1.434	7.540	0.005
BTV-F ≥ 51.15	2.987	1.314	6.793	0.009
BTLG-F ≥ 232.15	1.838	0.825	4.097	0.136

GS Total Gleason score total. OR odds ratio. CI confidence interval. T Total. P Prostate. L Lymph node. B Bone. V Visseral

MTV and PSMA SUVmean were identified as potential biomarkers of OS. However, TTV-P level was not found to be a prognostic factor for OS (36). In our study, the TTL-G + P ≥ 855.78 (95% CI: 4.878–1037.860, p = 0.006) value that we obtained by summing ¹⁸F-FDG PET/CT and ⁶⁸Ga-PSMA PET/CT parameters was found to be an independent prognostic factor for short OS. A cut-off value for TTL-G + P has not been found in the literature.

Whitney et al. suggested that age was a prognostic factor for OS in mCRPC, but did not define a threshold (37). However, Guijarro et al. showed in their study that there was no significant correlation between age and OS and PFS in patients with metastatic PC (38). Similarly, in our study, we did not find an association between age and OS in the univariate analysis.

Table 5 Multivariate cox regression analysis for OS

	P	OR	95.0% CI	
			Lower	Upper
Lscore ≥ 3	0.164	2.856	0.652	12.515
Vscore ≥ 3	< 0.001	26.355	7.069	98.251
TTV-P	0.361	2.534	0.345	18.613
TTL-P	0.381	2.167	0.384	12.228
TTV-F	0.564	0.324	0.007	14.815
TTL-G	0.095	0.129	0.012	1.425
TTV-P + F	0.162	0.034	0.000	3.922
TTL-G + P	0.006	224.225	4.878	10,307.860
LTV-F	0.569	0.464	0.033	6.512
LFDG-SUVmax	0.918	0.000	0.000	2.58E + 93
LFDG-SUVmean	0.911	264.693.642	0.000	7.18E + 103
BTV-F	0.108	3.112	0.780	12.418

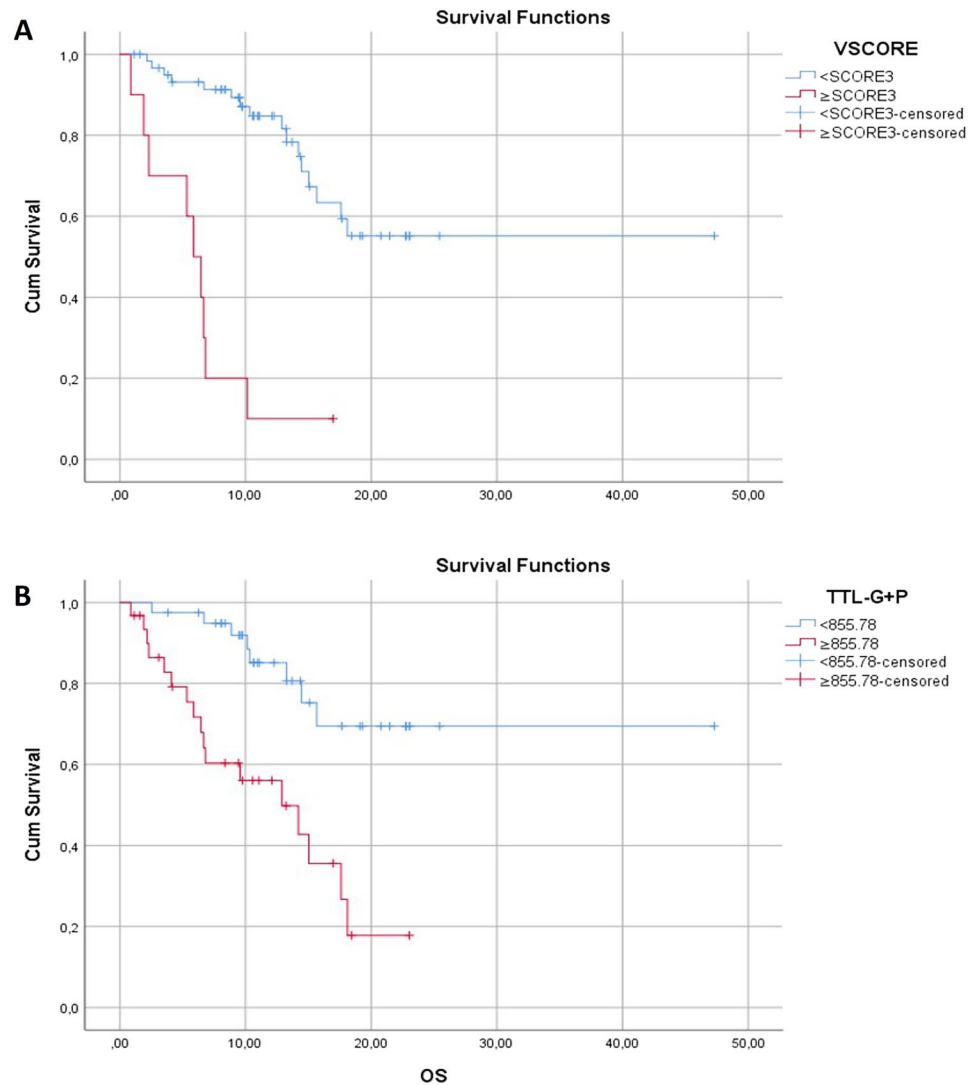
T Total. L Lymph node. B Bone, V Visseral, OR odds ratio, CI confidence interval

There are several studies that have reported that GS and serum PSA level are associated with OS in patients with PC. Oruç et al. found that especially baseline PSA and ΔPSA levels were independent prognostic factors for OS in patients with mCRPC receiving second-generation AR axis targeted therapy (23). Although several studies reported that patients with lower levels of serum PSA level had better OS, this parameter was not associated with OS (24, 25, 34). However, Ferdinandus et al. found no correlation between PSA level and OS (36). In our study, univariate Cox regression analysis showed no significant correlation between GS and serum PSA levels and OS.

Several studies have shown that the presence of visceral organ metastases in patients with PC is associated with a poor prognosis (37–41). An immunohistochemical study showed that membranous PSMA expression in PC metastases without neuroendocrine differentiation was significantly lower in liver metastases than in bone and lymph node metastases (6).

Several studies have shown that volumetric parameters obtained from ¹⁸F-FDG PET/CT and ⁶⁸Ga-PSMA PET/CT and score-based assessments showing increased glucose uptake may indicate tumor differentiation and contribute to disease management (42–44). In our study,

Fig. 2 Kaplan–Meier curves of overall survival according to (A) Vscore and (B) TTL-G+P



which was different in terms of design, $L_{\text{score}} \geq 3$ and $V_{\text{score}} \geq 3$ were found to be prognostic factors in predicting OS. In addition, in the multivariate analyses, a V_{score} of ≥ 3 was found to be an independent prognostic factor for short OS. Summarizing our findings, increased FDG uptake in lymph node and especially visceral organ metastases were associated with poor prognosis.

In light of the existing literature and the findings of our study, ^{18}F -FDG PET/CT and ^{68}Ga -PSMA PET/CT findings show that increased glucose uptake may predict a prognosis where the disease transforms into aggressive PC. Therefore, we recommend the use of dual tracer PET/CT in routine clinical practice in order to determine which group of patients will or will not benefit from treatment, and consequently, the approach to combined therapies.

Strengths and limitations

The main limitation of our study is its retrospective and single-centre design. The second limitation is the lack of secondary biopsy in patients after progression to mCRPC. Another limitation is that the association of OS within the already small group of patients with visceral metastases was not compared between organs. A further limitation is that it was not possible to compare the two different taxane treatments due to a lack of patients. On the other hand, the homogeneous group of patients receiving only taxane treatment is the strength of our study.

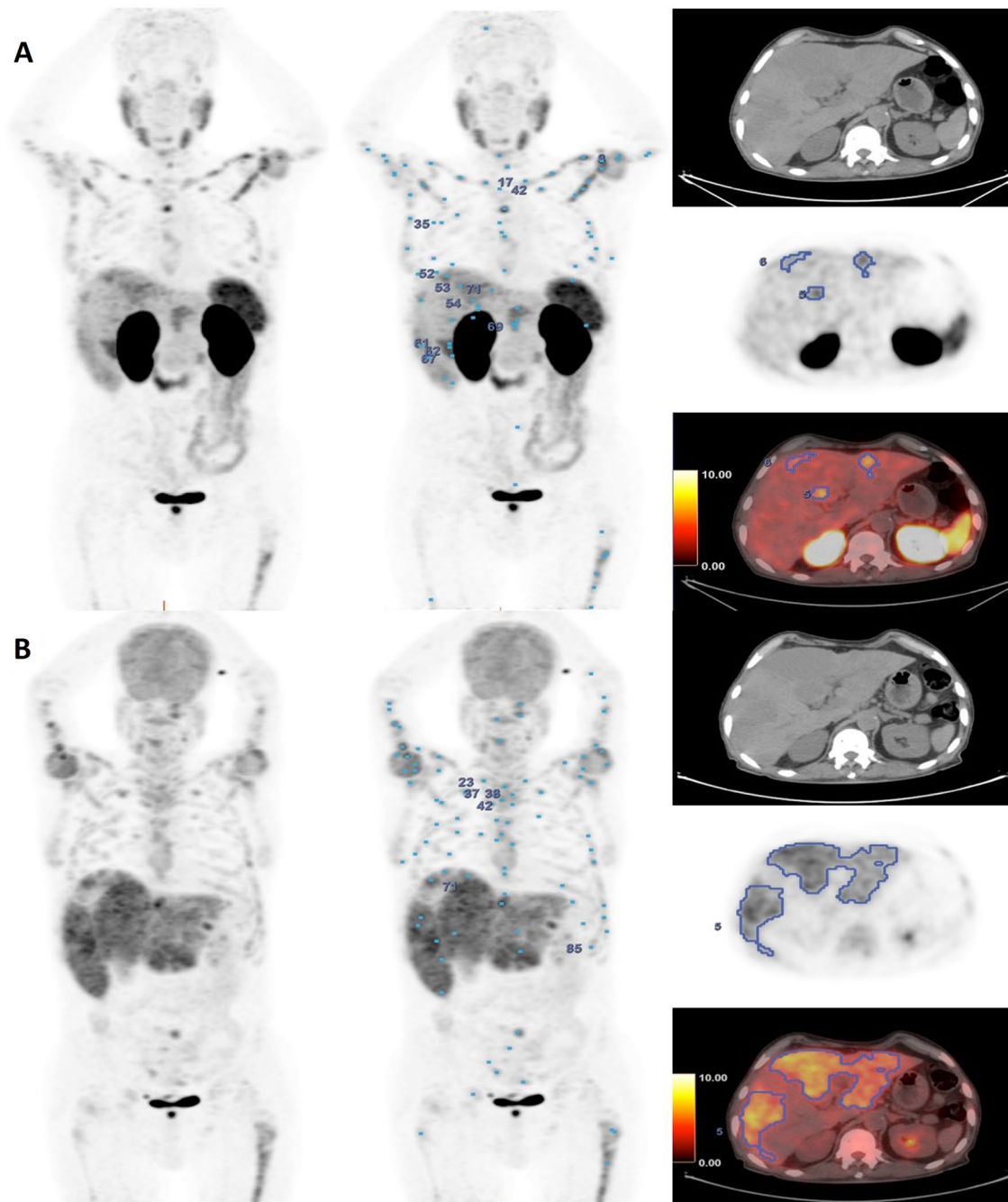


Fig. 3 A 69-year-old mCRPC (Gleason skor:4+5, TPSA:1129) patient with visceral score:5 and TTL-G+P: 9603.9 g/ml x cm³; ^{68}Ga -PSMA PET/CT A TTV-P: 610.2 cm³, TTL-P: 1415.4 g/ml x cm³ (MIP, PET and fusion image with and without VOIs) and ^{18}F -

FDG PET/CT B TTV-F: 1990.2 cm³, TTL-G: 8188.5 g/ml x cm³ (MIP, PET and fusion image with and without VOIs). The patient was given 6 cycles of cabazitaxel after imaging and the survival time was 5 months

Conclusion

We observed strong associations between OS and volumetric biomarkers derived from ^{68}Ga -PSMA PET/CT and ^{18}F -FDG PET/CT imaging and Pro-PET scores in patients with mCRPC receiving taxane group therapies. ^{18}F -FDG PET/CT

provides prognostic information when used in combination with ^{68}Ga -PSMA PET/CT in patients with mCRPC. This finding may open a new window into the characterisation of mCRPC heterogeneity, allowing for individualised therapy. Prospective studies involving a larger number of patients treated with both taxanes and non-taxanes are needed.

Funding None.

Data availability The findings and analysis sets of this study are available from the corresponding author upon reasonable request.

Declarations

Conflict of interest There no conflicts of interest.

References

- Siegel RL, Miller KD, Wagle NS, Jemal A. Cancer statistics, 2023. *CA Cancer J Clin*. 2023;73:17–48.
- Harris WP, Mostaghel EA, Nelson PS, Montgomery B. Androgen deprivation therapy: progress in understanding mechanisms of resistance and optimizing androgen depletion. *Nat Clin Pract Urol*. 2009;6:76–85 (Erratum in: *Nat Clin Pract Urol*. 2009;6:173).
- Watson PA, Arora VK, Sawyers CL. Emerging mechanisms of resistance to androgen receptor inhibitors in prostate cancer. *Nat Rev Cancer*. 2015;15:701–11.
- Wright GL Jr, Haley C, Beckett ML, Schellhammer PF. Expression of prostate-specific membrane antigen in normal, benign, and malignant prostate tissues. *Urol Oncol*. 1995;1:18–28.
- Bagguley D, Ong S, Buteau JP, Koschel S, Dhiantravan N, Hoffman MS, et al. Role of PSMA PET/CT imaging in the diagnosis, staging and restaging of prostate cancer. *Future Oncol*. 2021;17:2225–41.
- Paschalis A, Sheehan B, Riisnaes R, Rodrigues DN, Gurel B, Bertan C, et al. Prostate-specific membrane antigen heterogeneity and DNA repair defects in prostate cancer. *Eur Urol*. 2019;76:469–78.
- Eidelman E, Twum-Ampofo J, Ansari J, Siddiqui MM. The metabolic phenotype of prostate cancer. *Front Oncol*. 2017;7:131.
- Wang J, Xu W, Wang B, Lin G, Wei Y, Abudurexiti M, et al. GLUT1 is an AR target contributing to tumor growth and glycolysis in castration-resistant and enzalutamide-resistant prostate cancers. *Cancer Lett*. 2020;485:45–55.
- Fox JJ, Gavane SC, Blanc-Autran E, Nehmeh S, Gönen M, Beattie B, et al. Positron emission tomography/computed tomography-based assessments of androgen receptor expression and glycolytic activity as a prognostic biomarker for metastatic castration-resistant prostate cancer. *JAMA Oncol*. 2018;4:217–24.
- Petrylak DP, Tangen CM, Hussain MH, Lara PN Jr, Jones JA, Taplin ME, et al. Docetaxel and estramustine compared with mitoxantrone and prednisone for advanced refractory prostate cancer. *N Engl J Med*. 2004;351:1513–20.
- de Bono JS, Oudard S, Ozguroglu M, Hansen S, Machiels JP, et al. TROPIC investigators. prednisone plus cabazitaxel or mitoxantrone for metastatic castration-resistant prostate cancer progressing after docetaxel treatment: a randomised open-label trial. *Lancet*. 2010;376:1147–54.
- Fitzpatrick JM, de Wit R. Taxane mechanisms of action: potential implications for treatment sequencing in metastatic castration-resistant prostate cancer. *Eur Urol*. 2014;65:1198–204.
- Puente J, Grande E, Medina A, Maroto P, Lainez N, Arranz JA. Docetaxel in prostate cancer: a familiar face as the new standard in a hormone-sensitive setting. *Ther Adv Med Oncol*. 2017;9:307–18.
- Eiber M, Herrmann K, Calais J, Hadaschik B, Giesel FL, Hartenbach M, et al. Prostate cancer molecular imaging standardized evaluation (PROMISE): proposed miTNM classification for the interpretation of PSMA-ligand PET/CT. *J Nucl Med*. 2018;59:469–78.
- Fendler WP, Eiber M, Beheshti M, Bomanji J, Ceci F, Cho S, et al. 68Ga-PSMA PET/CT: Joint EANM and SNMMI procedure guideline for prostate cancer imaging: version 1.0. *Eur J Nucl Med Mol Imaging*. 2017;44:1014–24.
- Adnan A, Basu S. Concept proposal for a six-tier integrated dual tracer PET-CT (68Ga-PSMA and FDG) image scoring system (“Pro-PET” score) and examining its potential implications in metastatic castration-resistant prostate carcinoma theranostics and prognosis. *Nucl Med Commun*. 2021;42:566–74.
- Montironi R, Cimadamore A, Lopez-Beltran A, Scarpelli M, Aurilio G, Santoni M, et al. Morphologic, molecular and clinical features of aggressive variant prostate cancer. *Cells*. 2020;9:1073.
- Manucha V, Henegan J. Clinicopathologic diagnostic approach to aggressive variant prostate cancer. *Arch Pathol Lab Med*. 2020;144:18–23.
- Aparicio AM, Harzstark AL, Corn PG, Wen S, Araujo JC, Tu SM, et al. Platinum-based chemotherapy for variant castrate-resistant prostate cancer. *Clin Cancer Res*. 2013;19:3621–30.
- Vlachostergios PJ, Puca L, Beltran H. Emerging variants of castration-resistant prostate cancer. *Curr Oncol Rep*. 2017;19:32.
- Schmuck S, von Klot CA, Henkenberens C, Sohns JM, Christiansen H, Wester HJ, et al. Initial experience with volumetric 68Ga-PSMA I&T PET/CT for assessment of whole-body tumor burden as a quantitative imaging biomarker in patients with prostate cancer. *J Nucl Med*. 2017;58:1962–8.
- Grubmüller B, Rasul S, Baltzer P, Fajkovic H, D’Andrea D, Berndt F, et al. Response assessment using [68Ga]Ga-PSMA ligand PET in patients undergoing systemic therapy for metastatic castration-resistant prostate cancer. *Prostate*. 2020;80:74–82.
- Oruç Z, Güzel Y, Ebinç S, Kömek H, Küçüköner M, Kaplan MA, et al. Efficacy of 68Ga-PSMA PET/CT-derived whole-body volumetric parameters in predicting response to second-generation androgen receptor axis-targeted therapy, and the prognosis in metastatic hormone-refractory prostate cancer patients. *Nucl Med Commun*. 2021;42:1336–46.
- Can C, Gündoğan C, Yildirim OA, Poyraz K, Güzel Y, Kömek H. Role of 68Ga-PSMA PET/CT parameters in treatment evaluation and survival prediction in prostate cancer patients compared with biochemical response assessment. *Hell J Nucl Med*. 2021;24:25–35.
- Telli TA, Ozguven S, Alan O, Filizoglu N, Ozturk MA, Sariyar N, et al. Role of baseline 68Ga-PSMA PET/CT-derived whole-body volumetric parameters in predicting survival outcomes of metastatic castration-resistant prostate cancer patients receiving first-line treatment. *Ann Nucl Med*. 2022;36:964–75.
- Seifert R, Kessel K, Schlack K, Weber M, Herrmann K, Spanke M, et al. PSMA PET total tumor volume predicts outcome of patients with advanced prostate cancer receiving [177Lu]Lu-PSMA-617 radioligand therapy in a bicentric analysis. *Eur J Nucl Med Mol Imaging*. 2021;48:1200–10.
- Warburg O. On the origin of cancer cells. *Science*. 1956;123:309–14.
- Mueckler M, Thorens B. The SLC2 (GLUT) family of membrane transporters. *Mol Aspects Med*. 2013;34:121–38.
- Gallamini A, Zwarthoed C, Borra A. Positron emission tomography (PET) in oncology. *Cancers (Basel)*. 2014;6:1821–89.
- Jadvar H. Imaging evaluation of prostate cancer with 18F-fluorodeoxyglucose PET/CT: utility and limitations. *Eur J Nucl Med Mol Imaging*. 2013;40:5–10.
- Scafoglio C, Hirayama BA, Kepe V, Liu J, Ghezzi C, Satyamurthy N, et al. Functional expression of sodium-glucose transporters in cancer. *Proc Natl Acad Sci U S A*. 2015;112:E4111–9.

32. Liu Y, Cao Y, Zhang W, Bergmeier S, Qian Y, Akbar H, et al. A small-molecule inhibitor of glucose transporter 1 downregulates glycolysis, induces cell-cycle arrest, and inhibits cancer cell growth in vitro and in vivo. *Mol Cancer Ther*. 2012;11:1672–82.
33. Gonzalez-Menendez P, Hevia D, Mayo JC, Sainz RM. The dark side of glucose transporters in prostate cancer: Are they a new feature to characterize carcinomas? *Int J Cancer*. 2018;142:2414–24.
34. Bauckneht M, Bertagna F, Donegani MI, Durmo R, Miceli A, De Biasi V, et al. The prognostic power of 18F-FDG PET/CT extends to estimating systemic treatment response duration in metastatic castration-resistant prostate cancer (mCRPC) patients. *Prostate Cancer Prostatic Dis*. 2021;24:1198–207.
35. Wibmer AG, Morris MJ, Gonen M, Zheng J, Hricak H, Larson S, et al. Quantification of metastatic prostate cancer whole-body tumor Burden with ¹⁸F-FDG PET parameters and associations with overall survival after first-line abiraterone or enzalutamide: a single-center retrospective cohort study. *J Nucl Med*. 2021;62:1050–6.
36. Ferdinandus J, Violet J, Sandhu S, Hicks RJ, Ravi Kumar AS, Iravani A, et al. Prognostic biomarkers in men with metastatic castration-resistant prostate cancer receiving [¹⁷⁷Lu]-PSMA-617. *Eur J Nucl Med Mol Imaging*. 2020;47:2322–7.
37. Whitney CA, Howard LE, Posadas EM, Amling CL, Aronson WJ, Cooperberg MR, et al. In men with castration-resistant prostate cancer, visceral metastases predict shorter overall survival: what predicts visceral metastases? Results from the SEARCH database. *Eur Urol Focus*. 2017;3:480–6.
38. Guijarro A, Hernández V, de la Morena JM, Jiménez-Valladolid I, Pérez-Fernández E, de la Peña E, Llorente C. Influence of the location and number of metastases in the survival of metastatic prostatic cancer patients. *Actas Urol Esp*. 2017;41:226–33.
39. Mazzone E, Preisser F, Nazzani S, Tian Z, Bandini M, Gandaglia G, et al. Location of metastases in contemporary prostate cancer patients affects cancer-specific mortality. *Clin Genitourin Cancer*. 2018;16:376–84.e1.
40. Gandaglia G, Karakiewicz PI, Briganti A, Passoni NM, Schiffmann J, Trudeau V, et al. Impact of the site of metastases on survival in patients with metastatic prostate cancer. *Eur Urol*. 2015;68:325–34.
41. Xu N, Wu YP, Ke ZB, Liang YC, Tao X, Chen SH, et al. Risk factors of developing visceral metastases at diagnosis in prostate cancer patients. *Transl Cancer Res*. 2019;8:928–38.
42. Jadvar H. Molecular imaging of prostate cancer with 18F-fluorodeoxyglucose PET. *Nat Rev Urol*. 2009;6:317–23.
43. Wang B, Liu C, Wei Y, Meng J, Zhang Y, Gan H, et al. A Prospective trial of ⁶⁸Ga-PSMA and ¹⁸F-FDG PET/CT in nonmetastatic prostate cancer patients with an early PSA progression during castration. *Clin Cancer Res*. 2020;26(17):4551–8.
44. Kepenek F, Can C, Kömek H, Kaplan İ, Gündoğan C, Ebiç S, et al. Combination of [⁶⁸Ga] Ga-PSMA PET/CT and [¹⁸F] FDG PET/CT in demonstrating dedifferentiation in castration-resistant prostate cancer. *Médecine Nucléaire*. 2023. <https://doi.org/10.1016/j.mednuc.2022.12.001>.

Publisher's Note Springer Nature remains neutral with regard to jurisdictional claims in published maps and institutional affiliations.

Springer Nature or its licensor (e.g. a society or other partner) holds exclusive rights to this article under a publishing agreement with the author(s) or other rightsholder(s); author self-archiving of the accepted manuscript version of this article is solely governed by the terms of such publishing agreement and applicable law.